Welcome   Comments   Help

Origin of the $\phi \sim \pm 9°$ peaks in YBa$_2$Cu$_3$O$_{7-\delta}$ films grown on cubic zirconia substrates

D. G. Schlom
Department of Materials Science and Engineering, The Pennsylvania State University, University Park, Pennsylvania 16802-5005

E. S. Hellman, E. H. Hartford, Jr., and C. B. Eom[a)]
AT&T Bell Laboratories, Murray Hill, New Jersey 07974-0636

J. C. Clark
Department of Materials Science and Engineering, The Pennsylvania State University, University Park, Pennsylvania 16802-5005

J. Mannhart
IBM Research Division, Zurich Research Laboratory, CH-8803 Rüschlikon, Switzerland

The *c*-axis oriented YBa$_2$Cu$_3$O$_{7-\delta}$ films grown on (001) yttria-stabilized cubic zirconia (YSZ) substrates often contain domains whose in-plane alignment is rotated approximately 9° from the cube-on-cube epitaxial relationship, in addition to the more commonly observed 0° and 45° in-plane rotations. We have investigated the origin of this ∼9° orientation using *in situ* electron diffraction during growth and *ex situ* 4-circle x-ray diffraction. Our results indicate that the ∼9°orientation provides the most favorable lattice match between the interfacial (110)-oriented BaZrO$_3$ epitaxial reaction layer, which forms between YBa$_2$Cu$_3$O$_{7-\delta}$ and the YSZ substrate. If epitaxy occurs directly between YBa$_2$Cu$_3$O$_{7-\delta}$ and the YSZ substrate, i.e., before the BaZrO$_3$ epitaxial reaction layer is formed, the 0° and 45° domains have the most favorable lattice match. However, growth conditions that favor the formation of the BaZrO$_3$ reaction layer prior to the nucleation of YBa$_2$Cu$_3$O$_{7-\delta}$ lead to an increase in ∼9° domains. The observed phenomenon, which results from epitaxial alignment between the diagonal of a square surface net and the diagonal of a rectangular surface net, is a general method for producing in-plane misorientations, and has also been observed for the heteroepitaxial growth of other materials, including (Ba, K)BiO$_3$/LaAlO$_3$. The YBa$_2$Cu$_3$O$_{7-\delta}$/YSZ case involves epitaxial alignment between [$\bar{1}11$]$_{BaZrO_3}$ and [110]$_{YSZ}$, resulting in an expected in-plane rotation of 11.3° to 9.7° for fully commensurate and for fully relaxed (110)$_{BaZrO_3}$ on (001)$_{YSZ}$, respectively.

I. INTRODUCTION

Controlling the types and locations of grain boundaries between single crystals is not only useful for developing a detailed understanding of the effects of grain boundaries on the physical properties of a material, but in many instances it is useful for device purposes. Grain boundaries lie at the heart of many electroceramic devices, e.g., varistors, positive temperature coefficient (PTC) thermistors and internal-barrier-layer capacitors.[1] They influence the motion of domain boundaries in ferroelectrics and disrupt superconductivity in oxide superconductors, causing "weak links" and Josephson junctions. The ability to introduce grain boundaries of chosen

orientation at specific locations into epitaxial oxide films is thus very important for microelectronic applications. One example of grain boundary engineering is the "bi-epitaxy" process used to introduce 45° grain boundaries into epitaxial oxide superconductor films.[2,3] This process has been utilized to make superconducting quantum-interference devices (SQUID's).[4]

Just as it is important to engineer the location and orientation of introduced-grain boundaries, it is vital for many device applications to have the remaining regions free of grain boundaries. It is for these reasons that we studied the origin of the $\phi \sim 9°$ peaks observed[5–11] in x-ray diffraction studies of epitaxial films of YBa$_2$Cu$_3$O$_{7-\delta}$ grown with their *c*-axis aligned normal to the plane of the (001) yttria-stabilized cubic zirconia (YSZ) substrates (*c*-axis oriented YBa$_2$Cu$_3$O$_{7-\delta}$ films). Four-circle x-ray diffraction is often used to characterize the

[a)]Present address: Department of Mechanical Engineering and Materials Science, Duke University, Durham, North Carolina 27708-0300.

in-plane orientation of films. X-ray diffraction peaks at $\phi \sim 9°$ signify grain boundaries that, in their present uncontrolled state, are unwanted as they degrade the critical current density and microwave surface resistance of the superconducting YBa$_2$Cu$_3$O$_{7-\delta}$ film.[6,9,12–14] If understood and controllable, these $\sim 9°$ boundaries (and $45° - 9° = 36°$ grain boundaries) would be a significant improvement over 45° bi-epitaxy boundaries for many applications because of the higher critical current densities of the Josephson junctions formed at these lower-angle boundaries.

II. BACKGROUND

To clarify the lattice match discussions that follow, the crystal structures of YBa$_2$Cu$_3$O$_{7-\delta}$, YSZ, and BaZrO$_3$ are shown in Fig. 1 and their lattice parameters are given in Table I. YBa$_2$Cu$_3$O$_{7-\delta}$ has a layered perovskite-related structure, YSZ has the fluorite structure, and BaZrO$_3$ is a simple-cubic perovskite.

Multiple in-plane orientations have been reported in *c*-axis oriented YBa$_2$Cu$_3$O$_{7-\delta}$ films grown on (001)

FIG. 1. The crystal structures of YSZ, BaZrO$_3$, and YBa$_2$Cu$_3$O$_{7-\delta}$. Two equivalent representations of these crystal structures are shown: the atomic positions (above) and the coordination polyhedra (below). The oxygen atoms occupy the vertices of the coordination polyhedra. The relative sizes of the atoms reflect their relative ionic radii, as given by Ref. 15. The origins of the unit cells have been chosen to illustrate the similarities between the structures.

YSZ substrates.[3,5–11,14,19,20] The most common orientations observed are rotated 0° and 45° from the cube-on-cube orientation relationship. Specifically, the 0° in-plane rotation from cube-on-cube refers to

$$(001)_{\text{YBa}_2\text{Cu}_3\text{O}_{7-\delta}} \parallel (001)_{\text{YSZ}}$$
$$\text{and} \quad [100]_{\text{YBa}_2\text{Cu}_3\text{O}_{7-\delta}} \parallel [100]_{\text{YSZ}},$$

and the 45° in-plane rotation denotes

$$(001)_{\text{YBa}_2\text{Cu}_3\text{O}_{7-\delta}} \parallel (001)_{\text{YSZ}}$$
$$\text{and} \quad [110]_{\text{YBa}_2\text{Cu}_3\text{O}_{7-\delta}} \parallel [100]_{\text{YSZ}}.$$

The 45° in-plane rotation is typically dominant in films grown at lower substrate temperatures, while the 0° in-plane rotation is dominant for higher growth temperatures.[3,6,7] These two orientations have been understood in terms of the competition between surface mobility and lattice match.[6] The 45° in-plane rotation has a lattice mismatch[21] of about −5.7% with a near-coincident site surface mesh cell area of 0.14 nm². The 0° (cube-on-cube) in-plane rotation is better lattice matched, 0.1%, but the near-coincident site surface mesh cell area is much larger, 2.38 nm² Hence, under growth conditions where there is sufficient surface mobility (e.g., high substrate temperature), the dominant orientation relationship observed is the 0°, cube-on-cube, orientation relationship because of its lower lattic mismatch. Similarly, under conditions of low surface mobility, the 45° in-plane rotation is dominant. In addition, nucleation at surface steps on (001) YSZ substrates has been found to favor the 45° in-plane rotation,[9] an example of graphoepitaxy.

Besides these frequently observed orientations, in-plane rotations in the vicinity of 9° from the cube-on-cube orientation relationship have also been observed.[5–11] The first detailed report[7] of the $\phi \sim 9°$ peaks was accompanied by a possible explanation for their occurrence involving a near-coincident site lattice model.[7,8,11] However, no experimental evidence for such a mechanism has been reported, and our investigation of this phenomenon supports an alternative explanation, which is described below.[23] This alternate explanation was also independently proposed by Boikov
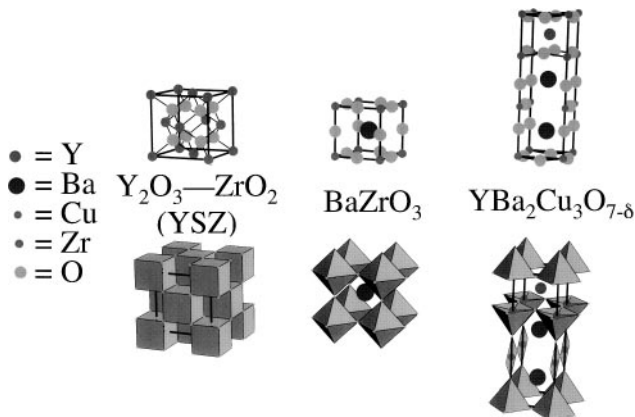
TABLE I. Lattice constants of YSZ, BaZrO$_3$, and YBa$_2$Cu$_3$O$_{7-\delta}$.

Material	Lattice constant(s) at 25 °C (Å)	Space group	Reference
(Y$_2$O$_3$)$_x$(ZrO$_2$)$_{1-x}$ (YSZ) ($x \approx 0.095$)	$a = 5.140$	$Fm3m$	16
BaZrO$_3$	$a = 4.193$	$Pm3m$	17
YBa$_2$Cu$_3$O$_{7-\delta}$ ($\delta \approx 0$)	$a = 3.820$ $b = 3.885$ $c = 11.68$	$Pmmm$	18
YBa$_2$Cu$_3$O$_{7-\delta}$ ($\delta \approx 1$)	$a = 3.857$ $c = 11.82$	$P4/mmm$	18

et al.,[10] although beyond suggesting this mechanism no supporting data was given. Here we present *in situ* characterization demonstrating the formation of a $\sim 9°$ in-plane-rotated (110)-oriented $BaZrO_3$ epitaxial reaction layer at the surfaces of (001) YSZ and (110) YSZ substrates exposed to BaO, and demonstrate that $\sim 9°$ in-plane rotations of $YBa_2Cu_3O_{7-\delta}$ grains occur on both of these YSZ substrate orientations at high substrate temperatures in agreement with or model. The formation of $\sim 9°$ in-plane-rotated domains in *c*-axis oriented $YBa_2Cu_3O_{7-\delta}$ films grown on (001) YSZ and (110) YSZ are examples of a general phenomena; examples of this same phenomena in the heteroepitaxial growth of other materials are also presented.

It has been widely shown that $YBa_2Cu_3O_{7-\delta}$ reacts with YSZ to form $BaZrO_3$,[24–28] and thin interfacial layers of $BaZrO_3$ are routinely observed between epitaxial $YBa_2Cu_3O_{7-\delta}$ films and the underlying YSZ substrates.[8,14,19,29–34] For the case of *c*-axis oriented $YBa_2Cu_3O_{7-\delta}$ films on (001) YSZ, both (001)-[8,14,19,33,34] and (110)-oriented[3,19,29,31] $BaZrO_3$ reaction layers have been seen at the $YBa_2Cu_3O_{7-\delta}$/YSZ interface by cross-sectional transmission electron microscopy (TEM).

In previous studies of 0° and 45° in-plane-rotated $YBa_2Cu_3O_{7-\delta}$ films grown on (001) YSZ substrates in which a $BaZrO_3$ epitaxial reaction layer has been seen, the researchers concluded that the $BaZrO_3$ layer formed *after* the orientation of the overlying $YBa_2Cu_3O_{7-\delta}$ layer was established.[19,34] In this paper we show that if the growth conditions are such that a $BaZrO_3$ epitaxial-reaction layer forms *before* the nucleation of the overlying $YBa_2Cu_3O_{7-\delta}$ layer, $\sim 9°$ in-plane rotations of the overlying $YBa_2Cu_3O_{7-\delta}$ layer are favored.

The orientation of the $BaZrO_3$ layers formed by epitaxial reaction is different depending on whether the $BaZrO_3$ is formed before or after the nucleation of the overlying $YBa_2Cu_3O_{7-\delta}$ layer. In the former unconstrained case, the $BaZrO_3$ is oriented (as we demonstrate below) with

$$(110)_{BaZrO_3} \parallel (001)_{YSZ} \quad \text{and} \quad [\bar{1}11]_{BaZrO_3} \parallel [110]_{YSZ},$$

whereas in the latter constrained case the $BaZrO_3$ is oriented with

$$(001)_{BaZrO_3} \parallel (001)_{YSZ}$$
$$\text{and} \quad [100]_{BaZrO_3} \parallel [100]_{YSZ},\text{[8,19,33,34]}$$

or

$$(001)_{BaZrO_3} \parallel (001)_{YSZ}$$
$$\text{and} \quad [110]_{BaZrO_3} \parallel [100]_{YSZ},\text{[8,14]}$$

or

$$(110)_{BaZrO_3} \parallel (001)_{YSZ}$$
$$\text{and} \quad [001]_{BaZrO_3} \parallel [100]_{YSZ}.\text{[19,31]}$$

The unconstrained orientation leads to in-plane rotations of $\sim 9°$, while the constrained orientations lead to 0° and 45° in-plane-rotated $YBa_2Cu_3O_{7-\delta}$ grains.

III. EXPERIMENTAL

Two orientations of YSZ substrates, (001) and (110), both containing 9.5 mol % Y_2O_3 [i.e., $(Y_2O_3)_{0.095}(ZrO_2)_{0.905}$] were used in this study.[35] Prior to growth the substrates were chem-mechanically polished,[36] degreased in acetone and alcohol, and mounted onto a substrate holder using silver paint for the sputtered samples or indium for the samples prepared by molecular beam epitaxy (MBE). The samples grown by off-axis pulsed laser deposition (PLD) were radiatively heated and loosely held by their sides, allowing both sides to be coated simultaneously. The $YBa_2Cu_3O_{7-\delta}$ layers were grown by dc hollow-cathode magnetron sputtering[37] and off-axis PLD.[38] The sputtered $YBa_2Cu_3O_{7-\delta}$ films were grown at a substrate heater block temperature of 750–780 °C, a total pressure ($Ar/O_2 = 2:1$) of 650 mTorr, and an after-growth cooldown in ~ 0.5 bar O_2 lasting ~ 1 h. Additional $YBa_2Cu_3O_{7-\delta}$ films were grown by off-axis PLD at a substrate temperature of 780 °C in 20 mTorr oxygen/ozone mixture ($\sim 5\%$ O_3) and an after-growth cooldown in 1 bar O_2 lasting ~ 1 h. The BaO and $(Ba, K)BiO_3$ layers were grown by MBE at substrate temperatures of 660–680 °C and 270–280 °C, respectively. An oxygen plasma generated in a tube (20 W rf power and an oxygen pressure of 90 mTorr) flowed into the MBE system, resulting in a background pressure of 5×10^{-5} to 10^{-4} Torr during growth.[39] The crystalline structure of the film surface was monitored by *in situ* reflection high-energy electron diffraction (RHEED) during growth. The $BaZrO_3$ films were grown by 90° off-axis magnetron sputtering at a substrate temperature of 650 °C and a total pressure of 100 mTorr ($Ar/O_2 = 3:2$).[40]

The orientation relationships between the $YBa_2Cu_3O_{7-\delta}$ films and YSZ substrates were determined using 4-circle x-ray diffraction in the Bragg–Brentano geometry and radiation from a copper x-ray tube. A schematic of the 4-circle geometry used is shown in Fig. 2. θ-2θ scans with the diffraction vector normal to the wafer surface were first used to establish which plane of the $YBa_2Cu_3O_{7-\delta}$ film lay parallel to the (001) YSZ substrate. This was the (001) $YBa_2Cu_3O_{7-\delta}$ plane for all of the growths discussed here (i.e., all are *c*-axis oriented $YBa_2Cu_3O_{7-\delta}$ films). Then ϕ-scans of $YBa_2Cu_3O_{7-\delta}$ 103 reflections were used to establish the
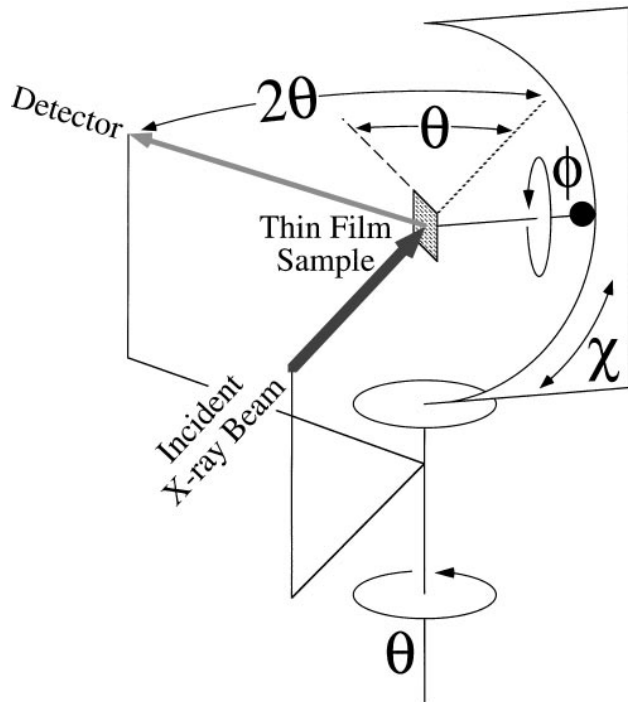
FIG. 2. A schematic diagram of a 4-circle x-ray diffractometer used to determine the epitaxial relationship between a film and a substrate.[41]

in-plane orientation relationship of the films with respect to the underlying substrate. As this is an inclined plane (asymmetric reflection), a component of the diffraction vector lies in the plane of the substrate. For all scans $\phi = 0°$ was set parallel to the [100] YSZ direction for (001) YSZ substrates and parallel to the [001] YSZ direction for (110) YSZ substrates. This in-plane direction ($\phi = 0°$) was ascertained from the location of the 011 YSZ reflection for (001) YSZ substrates and from the 100 YSZ reflection for (110) YSZ substrates. No distinction is made between the [100] YBa$_2$Cu$_3$O$_{7-\delta}$ and [010] YBa$_2$Cu$_3$O$_{7-\delta}$ directions in the x-ray scans nor in the deduced orientation relationships because the in-plane alignment of the [100] and [010] YBa$_2$Cu$_3$O$_{7-\delta}$ directions is determined during growth while the YBa$_2$Cu$_3$O$_{7-\delta}$ is tetragonal and the [100] and [010] YBa$_2$Cu$_3$O$_{7-\delta}$ directions are equivalent.

IV. RESULTS

In order to determine the origin of the $\phi \sim \pm 9°$ peaks in YBa$_2$Cu$_3$O$_{7-\delta}$ films grown on YSZ substrates, we begin by examining in detail the observation of Fork *et al.*[7] that the deposition of a thin (~ 0.3 nm) BaO buffer layer prior to YBa$_2$Cu$_3$O$_{7-\delta}$ deposition leads to a dominance of $\sim 9°$ in-plane-rotated YBa$_2$Cu$_3$O$_{7-\delta}$ grains. We present *in situ* RHEED characterization showing that the deposited BaO reacts with the YSZ substrate to form a $\sim 9°$ in-plane-rotated (110)-oriented

BaZrO$_3$ epitaxial reaction layer. This $\sim 9°$ in-plane-rotated epitaxial alignment occurs on both (001) YSZ and (110) YSZ substrates and involves the diagonal of a rectangular surface net aligning with the diagonal of a square surface net.

We then show that at high substrate temperatures c-axis oriented YBa$_2$Cu$_3$O$_{7-\delta}$ films grown on both (001) YSZ and (110) YSZ contain $\sim 9°$ in-plane-rotated YBa$_2$Cu$_3$O$_{7-\delta}$ domains. This implies that the $\sim 9°$ rotation of the YBa$_2$Cu$_3$O$_{7-\delta}$ domains is inherited from the underlying $\sim 9°$-rotated BaZrO$_3$ reaction layer; growth conditions (e.g., high substrate temperatures and low growth rates) favoring the formation of the $\sim 9°$-rotated BaZrO$_3$ reaction layer prior to the nucleation of the overlying YBa$_2$Cu$_3$O$_{7-\delta}$ lead to an increase in $\sim 9°$-rotated YBa$_2$Cu$_3$O$_{7-\delta}$ domains.

Finally, we consider the underlying general mechanism leading to this in-plane rotation. Ideal lattice constant ratios where this in-plane rotation provides the most favorable lattice match to a heteroepitaxial system are given and two additional examples of this general phenomenon, (110) (Ba, K)BiO$_3$/(001) YSZ and (110) (Ba, K)BiO$_3$/(001) LaAlO$_3$, are presented.

A. Epitaxial reaction between BaO and YSZ

Due to the dramatic ability of a thin BaO buffer layer to cause $\sim 9°$ in-plane rotations in the overgrown YBa$_2$Cu$_3$O$_{7-\delta}$ layer, as demonstrated by Fork *et al.*,[7] we began by examining the effect of such a thin BaO layer on the surface structure of (001) YSZ using *in situ* RHEED. Figure 3 shows the RHEED pattern observed at a $\sim 9°$ in-plane rotation off the [100] YSZ azimuth after the deposition of ~ 1.4 nm[42] of BaO on a (001) YSZ substrate at $T_{sub} \sim 665$ °C. The pattern cannot be indexed by BaO or YSZ reflections, but it can be by BaZrO$_3$ reflections. The RHEED pattern indicates the presence of a (110)-oriented BaZrO$_3$ epitaxial reaction layer with two different in-plane orientations: $[\bar{1}10]_{BaZrO_3}$ and $[001]_{BaZrO_3}$ parallel to the $\sim 9°$ off [100] YSZ azimuth. An identical RHEED patterns is observed at an in-plane rotation of $\sim 9°$ the other way from the [100] YSZ azimuth as well as at $\sim \pm 9°$ from the [010] YSZ azimuth. This indicates the presence of a total of four equivalent in-plane (110) BaZrO$_3$ orientations, as shown in Fig. 4(a). The lattice mismatch of these four equivalent orientation relationships is about -0.1% along the $[\bar{1}11]_{BaZrO_3} \parallel [110]_{YSZ}$ edge and 6.0% along the $[\bar{1}1\bar{2}]_{BaZrO_3} \parallel [1\bar{1}0]_{YSZ}$ edge of the near-coincident site surface mesh cell with area 0.77 nm^2, as shown for one of these equivalent orientations in Fig. 4(b). The observed orientation relationship between (110) BaZrO$_3$ and (001) YSZ has the most favorable lattice match of all possible near-coincident surface mesh cells of equal or smaller area.
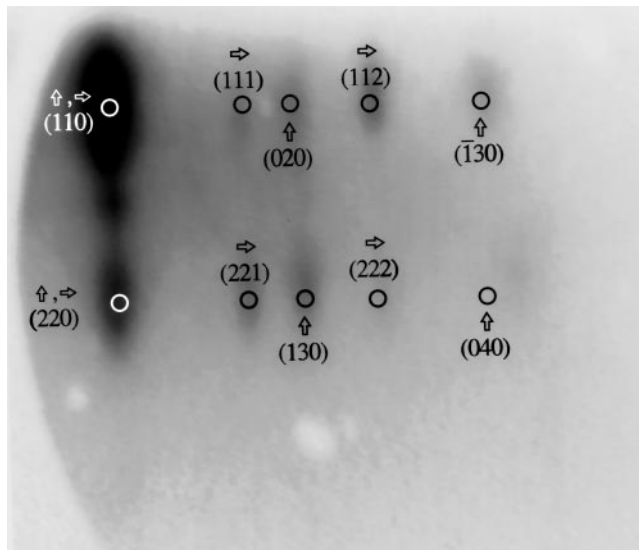
J. Mater. Res., Vol. 11, No. 6, Jun 1996

1339

FIG. 3. RHEED pattern observed $\sim 9°$ off the [100] YSZ azimuth after the deposition of 1.4 nm of BaO on (001) YSZ at $T_{sub} \sim 665$ °C. A superposition of two (110) BaZrO$_3$ orientations, $[\bar{1}10]_{BaZrO_3}$ BaZrO$_3$ azimuth (↑) and [001] BaZrO$_3$ azimuth (→), are indexed.

The in-plane rotation angle, ϕ, expected for these orientations was calculated from the lattice parameters of BaZrO$_3$ and YSZ for two limiting cases: (i) where the BaZrO$_3$ layer is strained to be fully commensurate with the underlying YSZ substrate and (ii) where the BaZrO$_3$ layer has fully relaxed. The result is ϕ values of $\pm 11.3°$ for fully commensurate and $\pm 9.7°$ for fully relaxed BaZrO$_3$ layers. As described below, it is this $\sim 9°$ in-plane rotation of the (110) BaZrO$_3$ layers that leads to the $\sim 9°$ in-plane rotation of the overgrown YBa$_2$Cu$_3$O$_{7-\delta}$ layers. Note that this angular value depends on the lattice constant of BaZrO$_3$. As significant ($\sim 10\%$) variations in the lattice constant of (110) BaZrO$_3$ epitaxial reaction layers on YSZ have been observed,[31] the peaks at $\sim \pm 9°$ observed in ϕ-scans of YBa$_2$Cu$_3$O$_{7-\delta}$ are in qualitatively good agreement with our expectations based on this orientation relationship.

The orientation relationship shown in Fig. 4 involves the epitaxial alignment between the diagonal of a square surface net and the diagonal of a rectangular surface net (specifically the epitaxial alignment between $\langle 111 \rangle_{BaZrO_3}$ and $\langle 110 \rangle_{YSZ}$). To test the generality of this epitaxial alignment, we also performed experiments on another orientation of YSZ containing an in-plane $\langle 110 \rangle$-type direction: (110) YSZ. In analogy to our results on (001) YSZ, we would expect the deposition of BaO on (110) YSZ to result in the formation of a (110)-oriented BaZrO$_3$ epitaxial reaction layer with

$$(110)_{BaZrO_3} \parallel (110)_{YSZ} \quad \text{and} \quad [\bar{1}11]_{BaZrO_3} \parallel [\bar{1}10]_{YSZ} .$$

The two equivalent ways in which $\langle 111 \rangle_{BaZrO_3}$ can align with $\langle 110 \rangle_{YSZ}$ in the nucleation of a (110) BaZrO$_3$
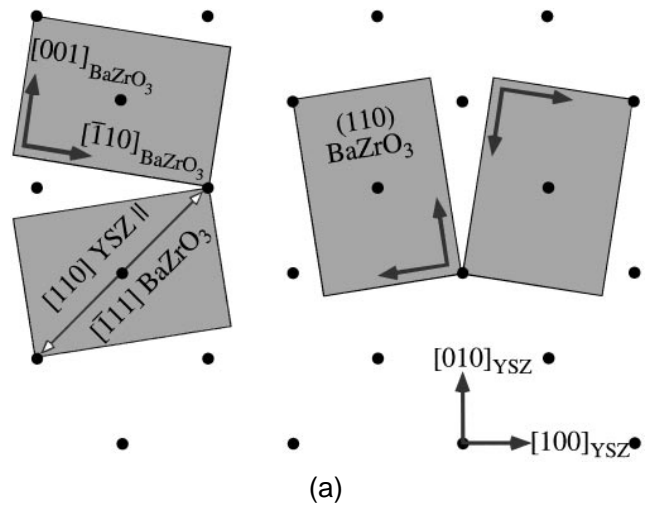
(a)
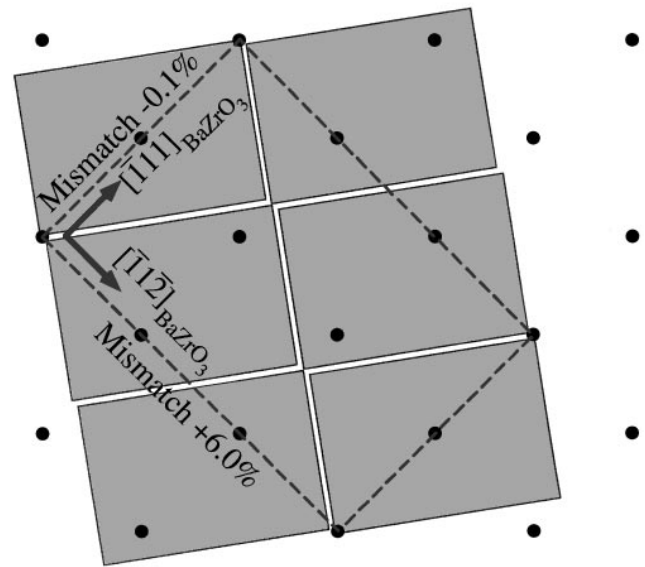
(b)

FIG. 4. Epitaxial relationship between (110) BaZrO$_3$ and (001) YSZ showing (a) the four equivalent domains with $[\bar{1}11]_{BaZrO_3} \parallel [110]_{YSZ}$ and (b) the near-coincident site surface mesh cell (dashed) and its lattice match for one of the four equivalent orientations. The rectangles indicate the relaxed dimensions of the (110) BaZrO$_3$ surface mesh with respect to the (001) YSZ substrate surface mesh (dots).

layer on (110) YSZ are shown in Fig. 5(a). As shown for one of these equivalent orientations in Fig. 5(b), the lattice mismatch of these orientation relationships is about -0.1% along both edges of the near-coincident site surface mesh cell with area 0.75 nm^2. This lattice match is even more favorable than that for (110) BaZrO$_3$ on (001) YSZ and is also the most favorable lattice match of all possible near-coincident surface mesh cells of equal or smaller area. This excellent lattice match results in the expected in-plane rotation angle, ϕ, between [001] BaZrO$_3$ and [001] YSZ to be
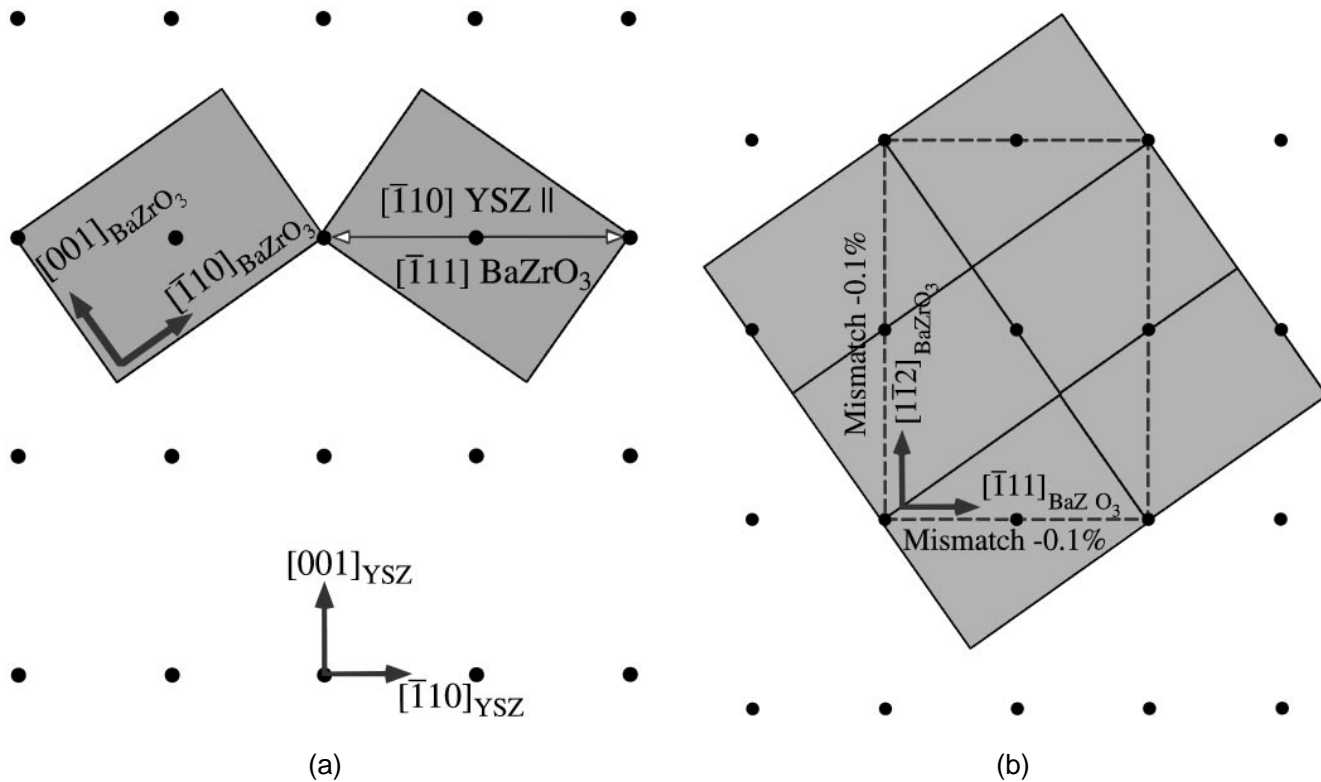
FIG. 5. Epitaxial relationship between (110) $BaZrO_3$ and (110) YSZ showing (a) the two equivalent domains with $[\bar{1}11]_{BaZrO_3} \parallel [\bar{1}10]_{YSZ}$ and (b) the near-coincident site surface mesh cell (dashed) and its lattice match for one of the two equivalent orientations. The rectangles indicate the relaxed dimensions of the (110) $BaZrO_3$ surface mesh with respect to the (110) YSZ substrate surface mesh (dots).

$\pm 35.3°$ regardless of whether the (110) $BaZrO_3$ layer is fully commensurate or fully relaxed.

The RHEED pattern observed along the [001] YSZ azimuth after the deposition of ~ 1.4 nm of BaO on (110) YSZ at $T_{sub} \sim 665$ °C is shown in Fig. 6. When viewed along the [001] $BaZrO_3$ azimuth ($\sim \pm 35°$ off the [001] YSZ azimuth) or the $[\bar{1}10]$ $BaZrO_3$ azimuth ($\sim \pm 125°$ off the [001] YSZ azimuth), the RHEED pattern looked identical to the corresponding $BaZrO_3$ azimuths shown superimposed in Fig. 3. The observed RHEED patterns are consistent with the orientation relationship shown in Fig. 5. Note that for the growth of (110) $BaZrO_3$ on (110) YSZ there are only two equivalent in-plane orientations because of the 2-fold symmetry of the substrate, compared to the four equivalent in-plane orientations on a (001) YSZ substrate.

B. $\phi \sim 9°$ peaks in $YBa_2Cu_3O_{7-\delta}$ on (001) YSZ

Having determined how a thin BaO buffer layer dramatically alters the surface structure of (001) YSZ and (110) YSZ substrates, Yielding a $\sim 9°$-rotated (110) $BaZrO_3$ layer, we now consider the origin of the $\sim 9°$ rotations observed in $YBa_2Cu_3O_{7-\delta}$ films grown on these substrates.

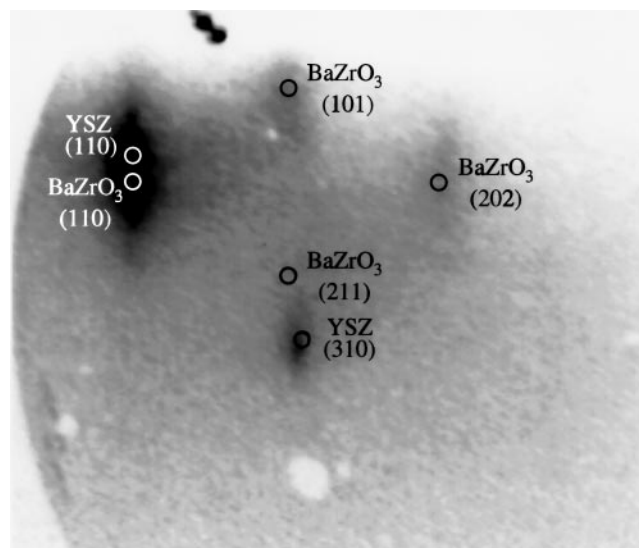In agreement with previous reports,[10,11] we found $\phi \sim 9°$ peaks to be most prevalent in $YBa_2Cu_3O_{7-\delta}$

FIG. 6. RHEED pattern observed along the [001] YSZ azimuth after the deposition of 1.4 nm of BaO on (110) YSZ at $T_{sub} \sim 665$ °C. Along this azimuth, both of the equivalent (110) $BaZrO_3$ orientations shown in Fig. 5 give rise to the same set of spots. These $BaZrO_3$ spots are indexed, as well as two spots due to the YSZ substrate.

films grown at high substrate temperatures. With increasing substrate temperature, the reaction between $YBa_2Cu_3O_{7-\delta}$ and YSZ occurs more rapidly, until at

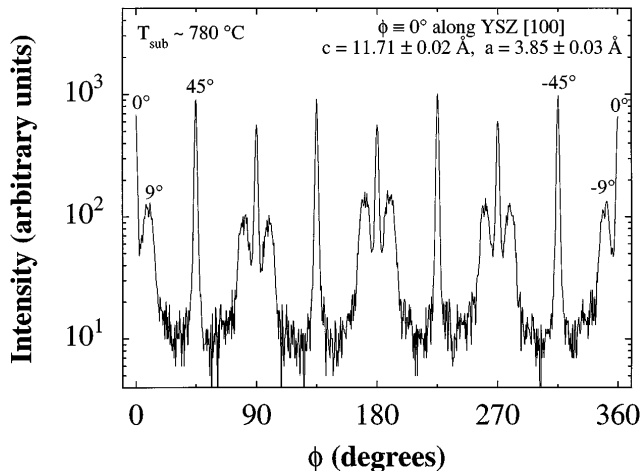FIG. 7. ϕ-scan of 103 YBa$_2$Cu$_3$O$_{7-\delta}$ peaks of *c*-axis oriented YBa$_2$Cu$_3$O$_{7-\delta}$ film grown on (001) YSZ grown by PLD at T_{sub} $\sim$ 780 °C.

some point the BaZrO$_3$ reaction layer forms *prior* to the nucleation of the YBa$_2$Cu$_3$O$_{7-\delta}$. The same event will occur at a fixed growth temperature as the growth rate is lowered, since the reaction then has more time to transpire. Such an event will lead to $\sim 9°$ in-plane rotations of (110) BaZrO$_3$ grains; the epitaxial sequence is identical to the BaO + YSZ case described above. Of course, microscopically there may be regions where the YBa$_2$Cu$_3$O$_{7-\delta}$ nucleates prior to the formation of BaZrO$_3$ and regions where BaZrO$_3$ nucleates prior to the YBa$_2$Cu$_3$O$_{7-\delta}$. In such cases, a mixture of 0°, 45°, and $\sim 9°$ in-plane rotations can be expected to occur. This is the typical observation for YBa$_2$Cu$_3$O$_{7-\delta}$ films grown on (001) YSZ substrates at high temperatures, an example of which is shown in Fig. 7.

The results of Fork *et al.*[7] on how thin BaO buffer layers deposited on YSZ (001) lead to a dramatic increase in $\sim 9°$ in-plane-rotated YBa$_2$Cu$_3$O$_{7-\delta}$ grains, together with the above *in situ* observations of the ensuing epitaxial reaction, indicate the full orientation relationship between the *c*-axis oriented YBa$_2$Cu$_3$O$_{7-\delta}$, the (110) BaZrO$_3$ epitaxial reaction layer, and the underlying (001) YSZ substrate is

$$(001)_{\text{YBa}_2\text{Cu}_3\text{O}_{7-\delta}} \parallel (110)_{\text{BaZrO}_3} \parallel (001)_{\text{YSZ}},$$
$$[100]_{\text{YBa}_2\text{Cu}_3\text{O}_{7-\delta}} \parallel [001]_{\text{BaZrO}_3},$$
$$\text{and} \quad [\bar{1}11]_{\text{BaZrO}_3} \parallel [110]_{\text{YSZ}}.$$

Cross-sectional TEM studies have shown that constrained (110)-oriented BaZrO$_3$, i.e., BaZrO$_3$ formed *after* the epitaxial alignment between YBa$_2$Cu$_3$O$_{7-\delta}$ and YSZ is established, epitaxially aligns with *c*-axis oriented YBa$_2$Cu$_3$O$_{7-\delta}$ in the following manner[19,31]:

$$(001)_{\text{YBa}_2\text{Cu}_3\text{O}_{7-\delta}} \parallel (110)_{\text{BaZrO}_3}$$
$$\text{and} \quad [110]_{\text{YBa}_2\text{Cu}_3\text{O}_{7-\delta}} \parallel [001]_{\text{BaZrO}_3}.$$

This orientation relationship is not the same as that inferred from the in-plane orientation of the $\sim 9°$ domains in *c*-axis YBa$_2$Cu$_3$O$_{7-\delta}$ films grown on (001) YSZ. The above orientation relationship would be manifested by peaks at $\phi \sim 36°$ and equivalent angles, rather than the observed peaks at $\phi \sim 9°$. Our *in situ* observations of the in-plane orientation of (110) BaZrO$_3$ on (001) YSZ together with the observation of peaks at $\phi \sim 9°$ and symmetrically equivalent angles indicate that the orientation relationship between unconstrained (110)-oriented BaZrO$_3$ and *c*-axis oriented YBa$_2$Cu$_3$O$_{7-\delta}$ is

$$(001)_{\text{YBa}_2\text{Cu}_3\text{O}_{7-\delta}} \parallel (110)_{\text{BaZrO}_3}$$
$$\text{and} \quad [100]_{\text{YBa}_2\text{Cu}_3\text{O}_{7-\delta}} \parallel [001]_{\text{BaZrO}_3}$$

on (001) YSZ substrates. Interestingly, both of these variants have *identical* lattice match[19] (2.6% and 8.8% mismatch along the surface mesh cell edge directions), as shown in Fig. 8. The near-coincident site surface mesh cell area is 0.94 nm^2 for the former orientation relationship and half this for the latter orientation relationship. Because of its smaller area,[43] the latter orientation relationship (indicated by peaks at $\phi \sim 9°$, rather than $\phi \sim 36°$) is dominant, as expected. As described below, sometimes both variants are seen in the same film, yielding not only peaks at $\phi \sim 9°$, but also peaks at $\phi \sim (45° - 9°) = 36°$.[11]

C. $\phi \sim 9°$ peaks in YBa$_2$Cu$_3$O$_{7-\delta}$ on (110) YSZ

In our model the origin of $\sim 9°$ in-plane-rotated YBa$_2$Cu$_3$O$_{7-\delta}$ domains is due to a $\sim 9°$-rotated (110) BaZrO$_3$ epitaxial reaction layer. As shown above (Fig. 5), a $\sim 9°$ in-plane-rotated (110) BaZrO$_3$ layer also occurs on (110) YSZ substrates. We thus investigated the growth of (001) YBa$_2$Cu$_3$O$_{7-\delta}$ on (110) YSZ to see if, at growth conditions favoring the formation of a BaZrO$_3$ reaction layer prior to the nucleation of the overlying YBa$_2$Cu$_3$O$_{7-\delta}$, in-plane rotation of the YBa$_2$Cu$_3$O$_{7-\delta}$ domains would also be observed, as predicted by our model.

The growth of *c*-axis oriented YBa$_2$Cu$_3$O$_{7-\delta}$ films has been reported on (001)-, (110)-, and (111)-oriented YSZ substrates as well as on misoriented YSZ substrates.[8,20,30,32,44] However, the in-plane orientation of YBa$_2$Cu$_3$O$_{7-\delta}$ deposited on (110) YSZ substrates has not been previously reported. As shown in Figs. 9 and 10, YBa$_2$Cu$_3$O$_{7-\delta}$ grows *c*-axis oriented with in-plane rotations of 0°, $\sim 9°$, and 45° on (110) YSZ. The relative fraction of these in-plane orientations depends on the substrate temperature during growth. At lower temperature, Fig. 10(a), the $\phi = 0°$ peaks dominate; at higher substrate temperature, Fig. 10(b), peaks at $\sim 9°$ and 45° are also observed. The 0° and 45° in-plane rotations are the orientations expected from lattice match considerations when YBa$_2$Cu$_3$O$_{7-\delta}$ nucleates
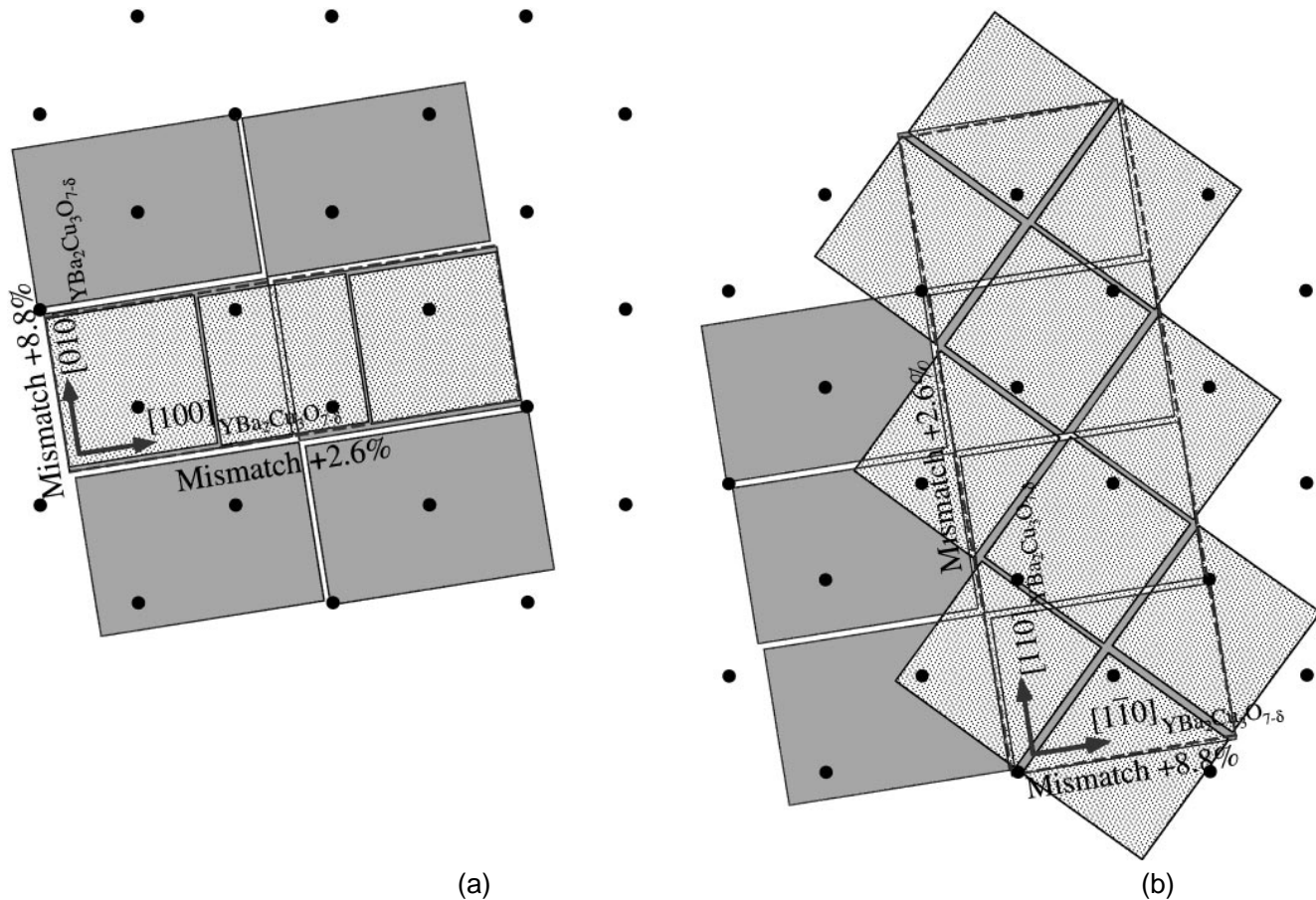
(a)
(b)

FIG. 8. Epitaxial relationship between (001) $YBa_2Cu_3O_{7-\delta}$ and (110) $BaZrO_3$ showing the near-coincident site surface mesh cell (dashed) and its lattice match for (a) $[010]_{YBa_2Cu_3O_{7-\delta}} \parallel [001]_{BaZrO_3}$, and (b) $[110]_{YBa_2Cu_3O_{7-\delta}} \parallel [001]_{BaZrO_3}$. The squares indicate the relaxed dimensions of the (001) $YBa_2Cu_3O_{7-\delta}$ surface mesh with respect to the (110) $BaZrO_3$ surface mesh (rectangles) on the (001) YSZ substrate surface mesh (dots).

directly on (110) YSZ. As shown in Fig. 11, the 0° relationship has a lattice mismatch of −5.7% along the $[100]_{YBa_2Cu_3O_{7-\delta}} \parallel [\bar{1}10]_{YSZ}$ edge and a mismatch of 0.1% along the $[010]_{YBa_2Cu_3O_{7-\delta}} \parallel [001]_{YSZ}$ edge of a near-coincident site surface mesh cell with area 0.58 nm². The 45° relationship has the identical lattice mismatch and near-coincident site surface mesh cell area: −5.7% along the $[110]_{YBa_2Cu_3O_{7-\delta}} \parallel [001]_{YSZ}$ edge, 0.1% along the $[1\bar{1}0]_{YBa_2Cu_3O_{7-\delta}} \parallel [\bar{1}10]_{YSZ}$ edge, and an area of 0.58 nm². However, if only the oxygen sublattice is considered, the 0° orientation relationship has a near-coincident site surface mesh cell area half the size (0.29 nm²) of the 45° orientation relationship, explaining the dominance of the 0° peaks compared to the 45° peaks in the ϕ-scans. The observation of more ∼9° peaks at higher substrate temperature is analogous to the growth of $YBa_2Cu_3O_{7-\delta}$ on (001) YSZ and expected from the increased likelihood of (110) $BaZrO_3$ formation before nucleation of the overlying $YBa_2Cu_3O_{7-\delta}$.

Combining the RHEED results indicating the epitaxial orientation of the (110) $BaZrO_3$ layer on (110) YSZ (see Fig. 5) with the ϕ-scan results [see Fig. 10(b)],
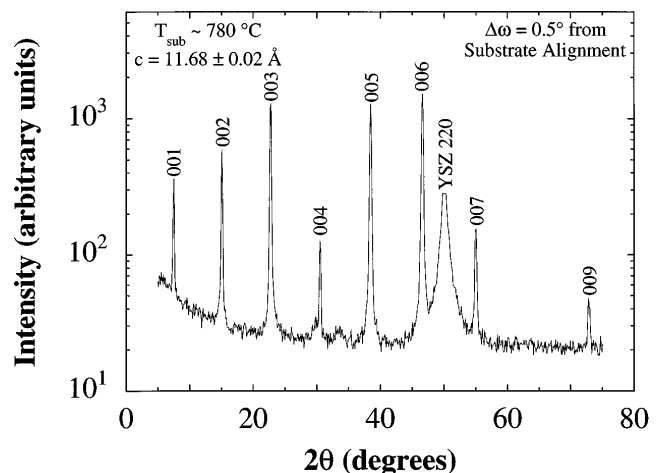
FIG. 9. θ-2θ scan of a *c*-axis oriented $YBa_2Cu_3O_{7-\delta}$ film grown on (110) YSZ by sputtering at $T_{sub} \sim 780$ °C. This scan was made after rocking 0.5° in omega off alignment to the (110) YSZ substrate.

the following orientation relationship is implied between the *c*-axis oriented $YBa_2Cu_3O_{7-\delta}$, the (110) $BaZrO_3$ epitaxial reaction layer, and the underlying (110) YSZ

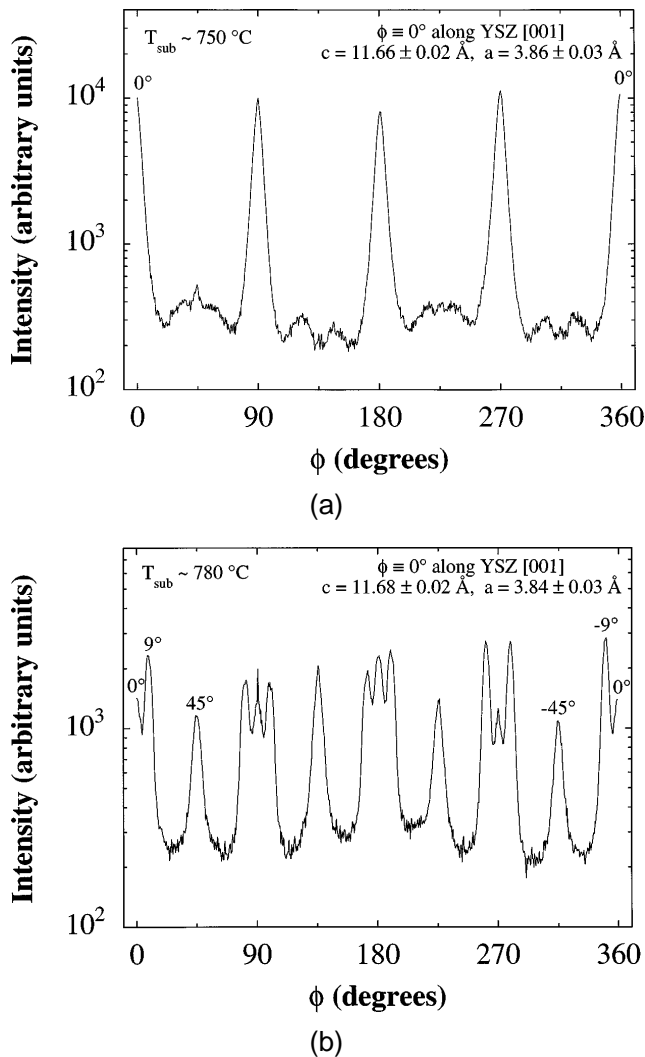FIG. 10. ϕ-scans of 103 YBa$_2$Cu$_3$O$_{7-\delta}$ peaks of *c*-axis oriented YBa$_2$Cu$_3$O$_{7-\delta}$ films grown on (110) YSZ by sputtering at (a) T_{sub} $\sim$ 750 °C and (b) T_{sub} $\sim$ 780 °C.

substrate:

$$(001)_{\text{YBa}_2\text{Cu}_3\text{O}_{7-\delta}} \parallel (110)_{\text{BaZrO}_3} \parallel (110)_{\text{YSZ}},$$
$$[110]_{\text{YBa}_2\text{Cu}_3\text{O}_{7-\delta}} \parallel [001]_{\text{BaZrO}_3},$$
$$\text{and} \quad [\bar{1}11]_{\text{BaZrO}_3} \parallel [\bar{1}10]_{\text{YSZ}} .$$

Note that the in-plane orientation between YBa$_2$Cu$_3$O$_{7-\delta}$ and BaZrO$_3$ differs by a 45° in-plane rotation from that observed on (001) YSZ. Although the lattice mismatch is identical for both of these orientation relationships, the reason for the preference of the variant with the larger near-coincident site surface mesh cell area[43] on (110) YSZ is unclear. In both cases, (001) YBa$_2$Cu$_3$O$_{7-\delta}$ is nucleating on (110) BaZrO$_3$. The clear dependence of the orientation relationship on the layer underlying the (110) BaZrO$_3$ [i.e., (001) YSZ or (110) YSZ] leads us to speculate that the step structure of the (110) BaZrO$_3$ layer, which is in turn dependent on the step structure of
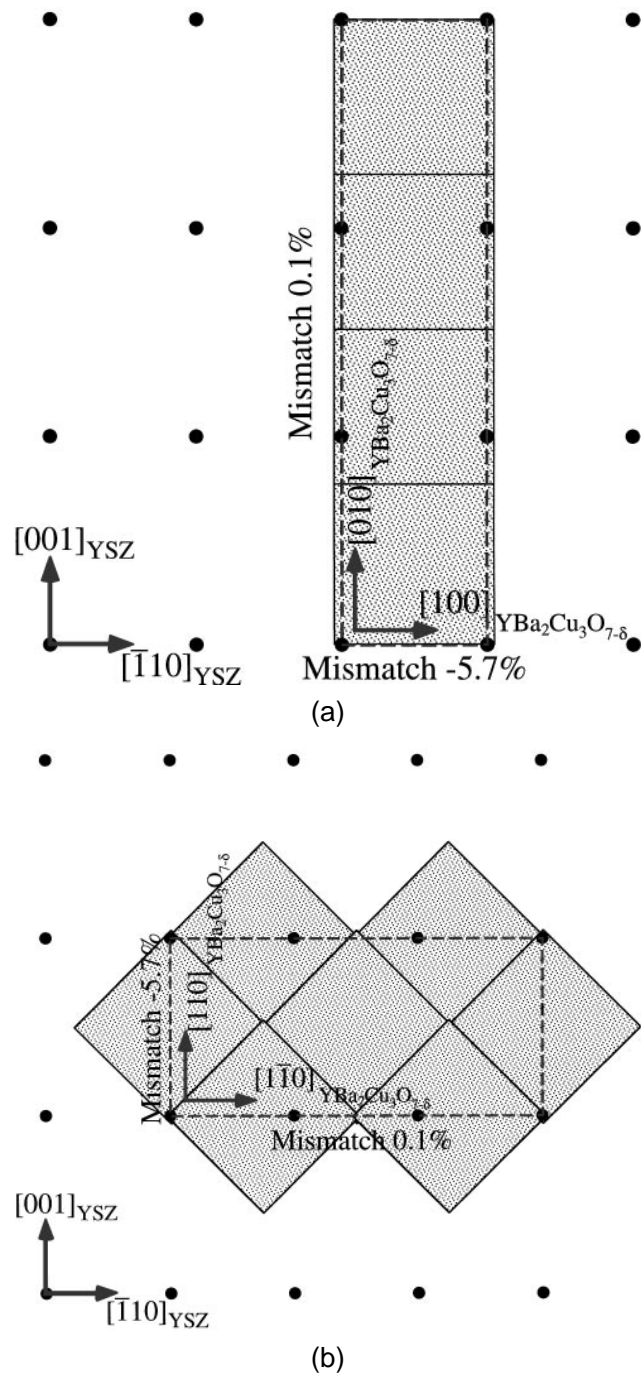
FIG. 11. Epitaxial relationship between (001) YB$_2$Cu$_3$O$_{7-\delta}$ and (110) YSZ showing the near-coincident site surface mesh cell (dashed) and its lattice match for (a) $[010]_{\text{YBa}_2\text{Cu}_3\text{O}_{7-\delta}} \parallel [001]_{\text{YSZ}}$ and (b) $[110]_{\text{YBa}_2\text{Cu}_3\text{O}_{7-\delta}} \parallel [001]_{\text{YSZ}}$. The squares indicate the relaxed dimensions of the (001) YBa$_2$Cu$_3$O$_{7-\delta}$ surface mesh with respect to the (110) YSZ substrate surface mesh (dots).

the underlying YSZ substrate orientation, is responsible for the dominance of one orientation relationship over the other. The importance of graphoepitaxy on the 45° in-plane orientation of (001) YBa$_2$Cu$_3$O$_{7-\delta}$ on (001) YSZ has been noted.[9] We believe that graphoepitaxy is also playing a role in the $\sim$9° in-plane orientation.

The in-plane orientation observations are in accord with our model and difficult to explain by other means. For example, just as a near-coincident site lattice model between (001) YBa$_2$Cu$_3$O$_{7-\delta}$ and (001) YSZ [i.e., without the prior formation of an intermediate (110) BaZrO$_3$ reaction layer] was inadequate to explain the occurrence of the $\sim 9°$ orientation,[11] it is also incapable of predicting $\sim 9°$ domains in (001) YBa$_2$Cu$_3$O$_{7-\delta}$ on (110) YSZ. The low-mismatch, low-Σ criterion used to select favorable orientations from near-coincident site lattices and meshes leads to the prediction that other orientations that are not seen should be observed, rather than the observed $\sim 9°$ in-plane-rotated orientation.

D. Other examples of general phenomenon

The formation of $\sim 9°$ in-plane-rotated domains in *c*-axis oriented YBa$_2$Cu$_3$O$_{7-\delta}$ films grown on (001) YSZ and (110) YSZ are just two examples of a general heteroepitaxial phenomenon. This phenomenon, involving the epitaxial alignment between the diagonal of a square surface mesh and the diagonal of a rectangular surface mesh, is a general method for producing in-plane misorientations. Here we describe the ideal lattice constant ratios where this phenomenon is expected to occur for a (110)/(001) interface between two cubic structures. Extension of this epitaxial alignment concept to the relevant surface meshes of other planes and lattices is straightforward. Additional examples of this phenomenon are then presented.

For a (110)-oriented film of a material with a simple cubic lattice with lattice constant a_{film} on a (001)-oriented substrate having a face-centered cubic (fcc) lattice with lattice constant $a_{\text{fcc sub}}$, this match along the diagonals occurs when $\sqrt{3}a_{\text{film}} = \sqrt{2}a_{\text{fcc sub}}$, or $a_{\text{film}} \cong 0.816\, a_{\text{fcc sub}}$. For comparison, the $a_{\text{film}}/a_{\text{fcc sub}}$ ratio for (110) BaZrO$_3$ on (001) YSZ is 0.816 (at room temperature). However, minimizing the mismatch along the diagonal does not minimize the lattice mismatch of the near-coincident site surface mesh. To minimize the latter, it is desired to minimize the lattice mismatch along two orthogonal directions, as can be seen from Fig. 4(b). The ideal lattice constant of the film (that minimizes the lattice match along two orthogonal directions) is attained when $a_{\text{film}} = 2\sqrt{3}(3\sqrt{2} - 4)a_{\text{fcc sub}}$, or $a_{\text{film}} \cong 0.841\, a_{\text{fcc sub}}$. Alternatively, if the (001)-oriented substrate has a simple cubic lattice with lattice constant a_{sub}, the corresponding value is $a_{\text{film}} = 4\sqrt{3}(3 - 2\sqrt{2})a_{\text{sub}}$, or $a_{\text{film}} \cong 1.189\, a_{\text{sub}}$. In both of these cases, the minimized lattice mismatch is 2.9% ($+2.9\%$ in one direction and -2.9% in the perpendicular direction).

A more favorable lattice match can be achieved along two orthogonal directions when this phenomenon occurs between a (110)-oriented film and a (110)-oriented substrate of two cubic materials. In this case, the ideal lattice constant of the film is attained in two orthogonal directions at the same time (i.e., perfect lattice match) when $a_{\text{film}} = \sqrt{2/3}a_{\text{fcc sub}}$, or $a_{\text{film}} \cong 0.816\, a_{\text{fcc sub}}$. As Fig. 5(b) shows, (110) BaZrO$_3$ on (110) YSZ is nearly this ideal case: $a_{\text{film}}/a_{\text{fcc sub}} = 0.816$ (at room temperature). Alternatively, if the (110)-oriented substrate has a simple cubic lattice, the ideal value is $a_{\text{film}} = (2/\sqrt{3})a_{\text{sub}}$, or $a_{\text{film}} \cong 1.155\, a_{\text{sub}}$.

From the above discussion, the ideal lattice parameter of a (110)-oriented simple cubic material for growth on (001) YSZ in order to observe this phenomenon is 4.319 Å. Ba$_{1-x}$K$_x$BiO$_3$ has a lattice constant of 4.322 Å to 4.287 Å over the composition range where its structure is simple cubic ($0.1 \lesssim x \lesssim 0.4$).[45,46] In hopes of observing another example of this phenomenon, involving the epitaxial alignment between the diagonal of a square surface mesh and the diagonal of a rectangular surface mesh, (110) (Ba, K)BiO$_3$ was grown on (001) YSZ. This growth was initiated at $T_{\text{sub}} \sim 550$ °C with the nucleation of BaBi$_x$O$_y$ ($x \sim 1$) for 5 min (~ 10 nm).[39,47]. Then the substrate temperature was lowered to ~ 270 °C and (Ba, K)BiO$_3$ was grown. As expected, sharp peaks at $\phi \sim \pm 9°$ were observed [see Fig. 12(a)]. Note, however, that the lattice parameter of (Ba, K)BiO$_3$ is quite close to that of BaZrO$_3$ (4.193 Å).[17] Although no x-ray diffraction peaks arising from (110) BaZrO$_3$ were detected, it is possible that an epitaxial reaction occurred between (Ba, K)BiO$_3$ and YSZ forming a thin (110) BaZrO$_3$ reaction layer, upon which the (Ba, K)BiO$_3$ layer subsequently grew.

An example of this same epitaxial phenomena between a simple cubic substrate and simple cubic film is (110) (Ba, K)BiO$_3$ on (001) LaAlO$_3$,[48] as shown in Fig. 12(b). Although the epitaxial alignment giving rise to the in-plane rotation is the same as that shown for YSZ in Fig. 4, here the peaks occur at $\phi \sim (45 - 9) = 36°$ because the LaAlO$_3$ surface mesh is not centered, resulting in a 45° rotation of the in-plane axes compared to the (001) YSZ surface mesh. The $a_{\text{film}}/a_{\text{sub}}$ ratio for (110) (Ba, K)BiO$_3$ on (001) LaAlO$_3$ is 1.13, compared to the ideal value of 1.189 discussed above.

V. DISCUSSION

Having investigated the origin of the $\phi \sim \pm 9°$ peaks, we reexamine the results presented by others related to $\sim 9°$ peaks in (001) YBa$_2$Cu$_3$O$_{7-\delta}$ films deposited on (001) YSZ. Our explanation, involving the epitaxial alignment between the diagonal of a square surface mesh and the diagonal of a rectangular surface mesh, is consistent with prior results and clarifies unexplained and previously unexpected observations. For example, Fork *et al.*[7] showed that the in-plane orientation of overlying YBa$_2$Cu$_3$O$_{7-\delta}$ layers was sensitively dependent on the deposition of extremely thin

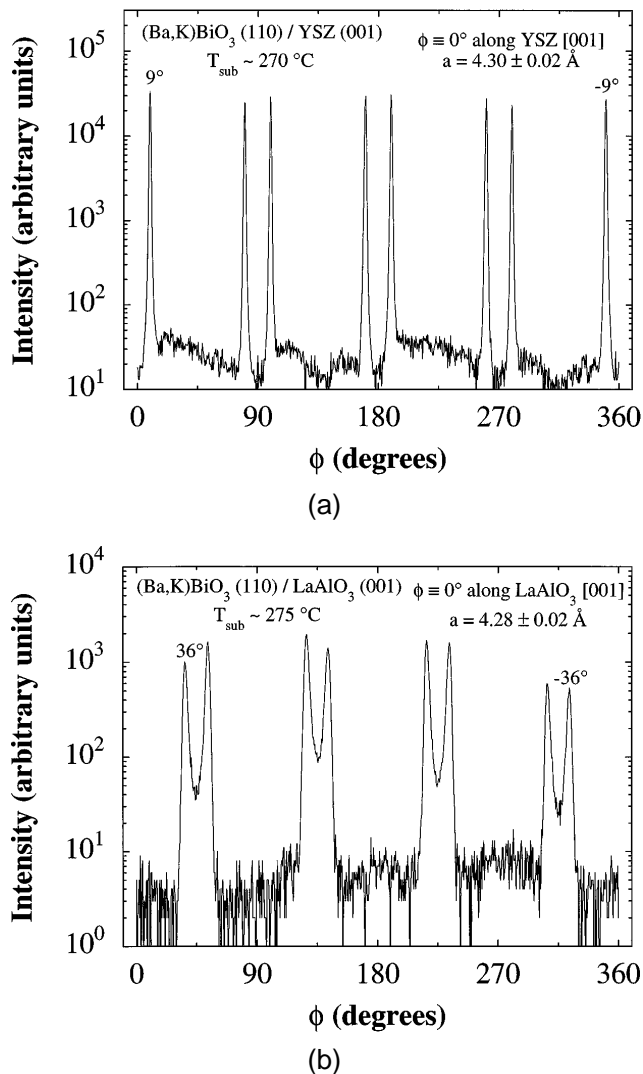FIG. 12. ϕ-scans of 200 $(Ba, K)BiO_3$ peaks of (110)-oriented $(Ba, K)BiO_3$ films grown by MBE on (a) (001) YSZ at $T_{sub} \sim 270$ °C and (b) (001) $LaAlO_3$ at $T_{sub} \sim 275$ °C.

layers ($\sim$0.3 nm) of BaO, CuO, Y_2O_3, or $BaZrO_3$ on (001) YSZ substrates, or on (001) YSZ substrates upon which a homoepitaxial YSZ layer was grown. The thin CuO, Y_2O_3, and $BaZrO_3$ layers and the homoepitaxial YSZ layer favored the 45° in-plane rotation, whereas the BaO layer led to the $\sim$9° in-plane rotation. Although this previous study lacked *in situ* characterization during the deposition of these thin layers, our *in situ* RHEED observations indicate the reason for the extreme sensitivity of the in-plane orientation to BaO deposition: it leads to a $\sim$9° rotated (110) $BaZrO_3$ epitaxial reaction layer, which subsequently determines the in-plane orientation of the $YBa_2Cu_3O_{7-\delta}$ overlayer. We have not studied the interfacial reactions of CuO or Y_2O_3 overlayers, but in contrast to the $BaO-ZrO_2$ case, the $CuO-ZrO_2$ phase diagram[49] is free of intermediate phases and the $Y_2O_3-ZrO_2$ phase diagram[50] not only

contains a very wide solid solution region (up to 40 mol % Y_2O_3), but the only intermediate compound,[50] $Zr_3Y_4O_{12}$, forms so sluggishly that single-phase YSZ films with up to 78 mol % Y_2O_3 have been reported.[51] Thus, of the thin layers deposited by Fork *et al.*,[7] an interfacial reaction layer is expected only for the case of BaO. The resultant (110)-oriented $BaZrO_3$ reaction layer subsequently leads to the dominant $\sim$9° in-plane rotation observed in the overgrown $YBa_2Cu_3O_{7-\delta}$ film.

Given the strong influence of the (110) $BaZrO_3$ interfacial reaction layer on the resulting in-plane orientation of the $YBa_2Cu_3O_{7-\delta}$, it may seem surprising that the thin $BaZrO_3$ layer deposited in the aforementioned study[7] did not also lead to $YBa_2Cu_3O_{7-\delta}$ domains with a $\sim$9° in-plane rotation. We attribute this to the growth of a non-(110) oriented $BaZrO_3$ layer. Fork *et al.*[7] did not report the orientation of their thin $BaZrO_3$ layers. However, we found that $BaZrO_3$ films *deposited* on (001) YSZ were mainly oriented in the cube-on-cube orientation, i.e., with (001) $BaZrO_3$ parallel to (001) YSZ, in contrast to the (110) $BaZrO_3$ orientation formed by epitaxial reaction. Others have reported (110)-oriented $BaZrO_3$ films deposited on (001) YSZ,[3,52] but they also report that the inverted interface, i.e., (001) YSZ deposited on (001) $BaZrO_3$, grows cube-on-cube.[3] As the epitaxial relationship obtained for the growth of $BaZrO_3$ on (001) YSZ and vice versa varies significantly with deposition conditions, it would appear from the absence of $\sim$9° domains in the $YBa_2Cu_3O_{7-\delta}$ films grown on top of a $BaZrO_3$ buffer layer by Fork *et al.*[7] that their $BaZrO_3$ layer was not (110)-oriented.

The predominant 45° in-plane rotation observed by Fork *et al.*[7] for $YBa_2Cu_3O_{7-\delta}$ films grown on (001) YSZ substrates with homoepitaxial YSZ buffer layers is consistent with the work of Brorsson *et al.*[9] Brorsson *et al.*[9] showed that homoepitaxial YSZ layers, grown under conditions similar to those used by Fork *et al.*,[7] have an increased surface step density compared to the underlying YSZ substrate. They found that an increased step density on the surface of (001) YSZ, regardless of whether it was from a homoepitaxial YSZ film or a result of high temperature annealing of the substrate, led to an increased fraction of 45° in-plane-rotated $YBa_2Cu_3O_{7-\delta}$ grains in the overlying film. Brorsson *et al.*[9] interpreted this result to imply that step edges on (001) YSZ substrates act as favorable nucleation sites for 45°-oriented $YBa_2Cu_3O_{7-\delta}$.[9] Since no reactions between the thin ($\sim$0.3 nm) CuO and Y_2O_3 layers deposited by Fork *et al.*[7] on (001) YSZ are expected, an analogous surface roughening and graphoepitaxial mechanism may take place, leading to the observed increase in 45° in-plane-rotated $YBa_2Cu_3O_{7-\delta}$ grains for these buffer layers as well.

Similar to the growth temperature effect reported for the growth of $YBa_2Cu_3O_{7-\delta}$ on (001) YSZ,[10,11]

in our growths on (110) YSZ substrates, the $\phi \sim 9°$ domains were observed at higher growth temperatures. This is consistent with the epitaxial relationship of the YBa$_2$Cu$_3$O$_{7-\delta}$ layer being established after the formation of the BaZrO$_3$ interfacial layer. Lower growth temperatures were free of $\phi \sim 9°$ domains, consistent with the epitaxial relationship of the YBa$_2$Cu$_3$O$_{7-\delta}$ layer being established before the formation of the BaZrO$_3$ layer.

Wen *et al.*[8] present a cross-sectional TEM image (Fig. 6 in Ref. 8) of a BaZrO$_3$ epitaxial in-plane reaction product between (001) YBa$_2$Cu$_3$O$_{7-\delta}$ and (001) YSZ that appears to be close to the $\sim 9°$ rotation that we have seen by RHEED. Their cross-sectional TEM image is along the [100] YSZ zone axis, and they state that this substrate zone-axis is approximately parallel to the [331] direction of the BaZrO$_3$ layer. This is within 3.5° of the (irrational) direction in BaZrO$_3$ that lies parallel to [100] YSZ (see Fig. 4) for fully relaxed BaZrO$_3$. Unfortunately, Wen *et al.*[8] do not indicate if the BaZrO$_3$ layer is (110)-oriented. However, it is clear that it must be different than the (001)-oriented BaZrO$_3$ layers that are present in the remainder of their TEM images as {001} cannot be perpendicular to [331].

Recently peaks at $\phi \sim \pm 37°$ have also been reported in *c*-axis oriented YBa$_2$Cu$_3$O$_{7-\delta}$ films grown on (001) YSZ, indicating the presence of YBa$_2$Cu$_3$O$_{7-\delta}$ grains with in-plane rotations of about 37°.[11] These peaks are observed in films grown under conditions similar to those in which peaks at $\phi \sim 9°$ occur (i.e., high substrate temperatures). In fact, both the $\phi \sim 9°$ peaks and the $\phi \sim 37°$ peaks were observed in the same film by Skofronick *et al.*[11] The origin of these $\sim 37°$ in-plane-rotated grains is likely the same as that of the $\sim 9°$ rotated grains. *c*-axis oriented YBa$_2$Cu$_3$O$_{7-\delta}$ is known to align epitaxially with (110)-oriented BaZrO$_3$ in two manners, related by a 45° in-plane rotation. The first is

$$(001)_{\text{YBa}_2\text{Cu}_3\text{O}_{7-\delta}} \parallel (110)_{\text{BaZrO}_3}$$
$$\text{and} \quad [100]_{\text{YBa}_2\text{Cu}_3\text{O}_{7-\delta}} \parallel [001]_{\text{BaZrO}_3},$$

as we have found to be dominant for the nucleation of YBa$_2$Cu$_3$O$_{7-\delta}$ on BaZrO$_3$ on (001) YSZ, and the second is

$$(001)_{\text{YBa}_2\text{Cu}_3\text{O}_{7-\delta}} \parallel (110)_{\text{BaZrO}_3}$$
$$\text{and} \quad [110]_{\text{YBa}_2\text{Cu}_3\text{O}_{7-\delta}} \parallel [001]_{\text{BaZrO}_3}$$

as others[19,31] have observed for BaZrO$_3$ formed after the epitaxial alignment between YBa$_2$Cu$_3$O$_{7-\delta}$ and YSZ is established. We have found the second to be dominant for the nucleation of YBa$_2$Cu$_3$O$_{7-\delta}$ on BaZrO$_3$ on (110) YSZ. As discussed earlier, both of these orientation relationships have identical lattice match, and we speculate that the dominance of a particular one is due to a graphoepitaxial contribution. The presence of both $\sim 9°$ and $\sim 37°$ in-plane

rotations in the YBa$_2$Cu$_3$O$_{7-\delta}$ films of Skofronick *et al.*,[11] in contrast to the more frequent observation of solely $\phi \sim 9°$ peaks, provides further evidence that an influencing factor other than lattice match alone is active. The more frequent observation of the $\phi \sim 9°$ peaks compared to the $\phi \sim 37°$ (or $45° - 9° = 36°$) peaks indicates that the $[100]_{\text{YBa}_2\text{Cu}_3\text{O}_{7-\delta}} \parallel [001]_{\text{BaZrO}_3}$ orientation is dominant for the growth conditions most frequently used to deposit (001) YBa$_2$Cu$_3$O$_{7-\delta}$ on (001) YSZ.

VI. CONCLUSIONS

The epitaxial alignment between the diagonal of a square surface mesh and the diagonal of a rectangular surface mesh is a general method for producing in-plane misorientations. The model presented explains why diffraction peaks at $\phi \sim 9°$ are observed in *c*-axis oriented YBa$_2$Cu$_3$O$_{7-\delta}$ grown on (001) YSZ as well as on (110) YSZ substrates, and has been used to select other epitaxial systems to demonstrate this phenomenon. If a means could be found to suppress all but one of the $\sim 9°$ in-plane-rotated domains, this technique could provide a significant advantage in grain boundary engineering over the bi-epitaxy process for the growth of YBa$_2$Cu$_3$O$_{7-\delta}$-based and (Ba, K)BiO$_3$-based Josephson junctions.

REFERENCES

1. A. J. Moulson and J. M. Herbert, *Electroceramics: Materials • Properties • Applications* (Chapman & Hall, London, 1990).
2. K. Char, M. S. Colclough, S. M. Garrison, N. Newman, and G. Zaharchuk, Appl. Phys. Lett. **59**, 733 (1991); K. Char, M. S. Colclough, L. P. Lee, and G. Zaharchuk, Appl. Phys. Lett. **59**, 2177 (1991).
3. X. D. Wu, L. Luo, R. E. Muenchausen, K. N. Springer, and S. Foltyn, Appl. Phys. Lett. **60**, 1381 (1992).
4. L. P. Lee, K. Char, M. S. Colclough, and G. Zaharchuk, Appl. Phys. Lett. **59**, 3051 (1991).
5. D. K. Fork, A. Barrera, T. H. Geballe, A. M. Viano, and D. B. Fenner, Appl. Phys. Lett. **57**, 2504 (1990).
6. S. M. Garrison, N. Newman, B. F. Cole, K. Char, and R. W. Barton, Appl. Phys. Lett. **58**, 2168 (1991); S. M. Garrison, N. Newman, B. F. Cole, K. Char, and R. W. Barton, Appl. Phys. Lett. **59**, 3060 (1991).
7. D. K. Fork, S. M. Garrison, M. Hawley, and T. H. Geballe, J. Mater. Res. **7**, 1641 (1992).
8. J. G. Wen, C. Traeholt, H. W. Zandbergen, K. Joosse, E. M. C. M. Reuvekamp, and H. Rogalla, Physica C **218**, 29 (1993).

9. G. Brorsson, E. Olsson, Z. G. Ivanov, E. A. Stepantsov, J. A. Alarco, Y. Boikov, T. Claeson, P. Berastegui, V. Langer, and M. Löfgren, J. Appl. Phys. **75**, 7958 (1994).

10. Y. Boikov, Z. G. Ivanov, G. Brorsson, and T. Claeson, Supercond. Sci. Technol. **7**, 281 (1994).

11. G. L. Skofronick, A. H. Carim, S. R. Foltyn, and R. E. Muenchausen, J. Appl. Phys. **76**, 4753 (1994).

12. D. Dimos, P. Chaudhari, and J. Mannhart, Phys. Rev. B **41**, 4038 (1990).

13. S. S. Laderman, R. C. Taber, R. D. Jacowitz, J. L. Moll, C. B. Eom, T. L. Hylton, A. F. Marshall, T. H. Geballe, and M. R. Beasley, Phys. Rev. B **43**, 2922 (1991).

14. J. A. Alarco, G. Brorsson, Z. G. Ivanov, P-Å. Nilsson, E. Olsson, and M. Löfgren, Appl. Phys. Lett. **61**, 723 (1992).

15. R. D. Shannon, Acta Crystallogr. A **32**, 751 (1976).

16. R. P. Ingel and D. Lewis, III, J. Am. Ceram. Soc. **69**, 325 (1986).

17. JCPDS card 6-399 (JCPDS International Centre for Diffraction Data, Swarthmore, PA).

18. R. Beyers and T. M. Shaw, Solid State Phys. **42**, 135 (1989), and references therein.

19. G. L. Skofronick, A. H. Carim, S. R. Foltyn, and R. E. Muenchausen, J. Mater. Res. **8**, 2785 (1993).

20. C. H. Mueller, P. H. Holloway, J. D. Budai, F. A. Miranda, and K. B. Bhasin, J. Mater. Res. **10**, 810 (1995).

21. The lattice mismatch values given throughout this article are calculated by the formula $(a_{sub} - a_{film}/a_{film})$.[22] Although the lattice constants vary with temperature and composition ($0.095 \leqslant x \leqslant 0.6$ in $(Y_2O_3)_x(ZrO_2)_{1-x}$ and $0 \leqslant \delta \leqslant 1$ in YBa$_2$Cu$_3$O$_{7-\delta}$) and it would be most appropriate to report the lattice mismatch for the specific growth conditions used, for simplicity we report the lattice mismatch at room temperature, $x \sim 0.095$[16] and $\delta \sim 0$.[18] These approximate values are adequate for the relatively qualitative reasoning that lattice mismatch considerations allow.

22. See, for example, J. W. Matthews in *Epitaxial Growth, Part B*, edited by J. W. Matthews (Academic Press, New York, 1975), pp. 559–609.

23. D. G. Schlom, E. S. Hellman, E. H. Hartford, Jr., and J. Mannhart, presented at the Fall '93 Materials Research Society Meeting in Boston, MA, 1993 (unpublished).

24. J. J. Cuomo, M. F. Chisholm, D. S. Yee, D. J. Mikalsen, P. B. Madakson, R. A. Roy, E. Giess, and G. Scilla, in *Thin Film Processing and Characterization of High-Temperature Superconductors*, AIP Conference Proceedings No. 165, edited by J. M. E. Harper, R. J. Colton, and L. C. Feldman (American Institute of Physics, New York, 1988), pp. 141–148.

25. T. Komatsu, O. Tanaka, K. Matusita, M. Takata, and T. Yamashita, Jpn. J. Appl. Phys. **27**, L1025 (1988).

26. H. Koinuma, K. Fukuda, T. Hashimoto, and K. Fueki, Jpn. J. Appl. Phys. **27**, L1216 (1988).

27. M. J. Cima, J. S. Schneider, S. C. Peterson, and W. Coblenz, Appl. Phys. Lett. **53**, 710 (1988).

28. C. T. Cheung and E. Ruckenstein, J. Mater. Res. **4**, 1 (1989).

29. L. A. Tietz, C. B. Carter, D. K. Lathrop, S. E. Russek, R. A. Buhrman, and J. R. Michael, J. Mater. Res. **4**, 1072 (1989). The 0.3 nm fringe spacing reported for the intermediate reaction layer in the cross-sectional TEM image (identified as being possibly BaZrO$_3$) indicates that the BaZrO$_3$ is (110)-oriented.

30. M. J. Shapiro, K. L. More, W. J. Lackey, J. A. Hanigofsky, D. N. Hill, W. B. Carter, E. K. Barefield, E. A. Judson, D. F. O'Brien, R. Patrick, Y. S. Chung, and T. S. Moss, J. Am. Ceram. Soc. **74**, 2021 (1991).

31. D. M. Hwang, Q. Y. Ying, and H. S. Kwok, Appl. Phys. Lett. **58**, 2429 (1991).

32. M. J. Casanove, A. Alimoussa, C. Roucau, C. Escribe-Filippini, P. L. Reydet, and P. Marcus, Physica C **175**, 285 (1991).

33. O. Eibl, K. Hradil, and H. Schmidt, Physica C **177**, 89 (1991).

34. J. A. Alarco, G. Brorsson, H. Olin, and E. Olsson, J. Appl. Phys. **75**, 3202 (1994).

35. Ceres Corp., N. Billerica, Massachusetts.

36. Commercial Crystal Laboratories, Naples, Florida.

37. X. X. Xi, G. Linker, O. Meyer, E. Nold, B. Obst, F. Ratzel, R. Smithey, B. Strehlau, F. Weschenfelder, and J. Geerk, Z. Phys. B **74**, 13 (1989).

38. B. Holzapfel, B. Roas, L. Schultz, P. Bauer, and G. Saemann-Ischenko, Appl. Phys. Lett. **61**, 3178 (1992).

39. E. S. Hellman, E. H. Hartford, and E. M. Gyorgy, Appl. Phys. Lett. **58**, 1335 (1991).

40. C. B. Eom, J. Z. Sun, K. Yamamoto, A. F. Marshall, K. E. Luther, T. H. Geballe, and S. S. Laderman, Appl. Phys. Lett. **55**, 595 (1989).

41. L. V. Azároff, *Elements of X-Ray Crystallography* (McGraw-Hill, New York, 1968), pp. 360–389.

42. With the oxygen plasma on, the sample was exposed to the barium beam for 40 s. RBS measurement of the resulting BaO film thickness deposited on a comounted MgO substrate ($T_{sub} \sim 660$ °C) indicated an average BaO film thickness of 1.4 nm.

43. Note that depending on the surface termination of the (110) BaZrO$_3$ layer, the oxygen sublattice of this latter orientation relationship ($[110]_{YBa_2Cu_3O_{7-\delta}} \parallel [001]_{BaZrO_3}$) could have the *same* surface mesh area as the oxygen sublattice of the former orientation relationship ($[100]_{YBa_2Cu_3O_{7-\delta}} \parallel [001]_{BaZrO_3}$). There are two distinct (110) BaZrO$_3$ planes, neither of which is charge neutral: BaZrO and O$_2$. If the latter is the terminating layer, the oxygen sublattice of the near-coincident site surface mesh cell shown in Fig. 8 is centered, and the primitive cell would have an area of 0.47 nm^2.

44. C. Escribe-Filippini, P. L. Reydet, J. Marcus, and M. Burnel, J. Less-Comm. Met. **151**, 263 (1989).

45. L. F. Schneemeyer, J. K. Thomas, T. Siegrist, B. Batlogg, L. W. Rupp, R. L. Opila, R. J. Cava, and D. W. Murphy, Nature (London) **335**, 421 (1988).

46. J. P. Wignacourt, J. S. Swinnea, H. Steinfink, and J. B. Goodenough, Appl. Phys. Lett. **53**, 1753 (1988).

47. M. G. Norton, E. S. Hellman, E. H. Hartford, Jr., and C. B. Carter, Physica C **205**, 347 (1993); M. G. Norton, E. S. Hellman, E. H. Hartford, Jr., and C. B. Carter, J. Cryst. Growth **113**, 716 (1991).

48. *Landolt–Börstein: Numerical Data and Functional Relationships in Science and Technology, New Series*, Group III, Vol. 12a, edited by K-H. Hellwege (Springer-Verlag, Berlin, 1978), p. 160. At room temperature LaAlO$_3$ is rhombohedral (not simple cubic). However, the distortion from simple cubic is extremely small ($\alpha = 60.1°$) vs. $\alpha = 60°$ for cubic. Furthermore, at the substrate temperature at which growth was initiated, $T_{sub} \sim 550$ °C, LaAlO$_3$ is cubic.

49. A. M. M. Gadalla and J. White, Trans. Brit. Ceram. Soc. **65**, 383 (1966).

50. V. S. Stubican, R. C. Hink, and S. P. Ray, J. Am. Ceram. Soc. **61**, 17 (1978); V. S. Stubican and J. R. Hellmann, in *Science and Technology of Zirconia*, Vol. 3 in Advances in Ceramics series, edited by A. H. Heuer and L. W. Hobbs (American Ceramic Society, Westerville, OH, 1981), pp. 25–36.

51. H. Holzschuh and H. Suhr, Appl. Phys. Lett. **59**, 470 (1991).

52. D. K. Fork (private communication). These (110) BaZrO$_3$ films were deposited on (001) YSZ on (001) Si. They were much thicker than the ~ 0.3 nm BaZrO$_3$ buffer layers studied in Ref. 7. Interestingly, a ϕ-scan of these (110)-oriented BaZrO$_3$ films on (001) YSZ revealed two in-plane orientation variants rotated with respect to one another by 9.5°!